Biofuel Research Journal 34 (2022) 1617-1629

Biofuel Research Journal

Journal homepage: www.biofueljournal.com

Original Research Paper

Fractionation of fatty acid methyl esters *via* urea inclusion and its application to improve the low-temperature performance of biodiesel

Junli Liu*, Bernard Tao

Agricultural and Biological Engineering Department, Purdue University, West Lafayette, IN 47907, USA.

HIGHLIGHTS

- Supersaturation of urea in solution regulates the urea inclusion fractionation process.
- The yield loss can be minimized through hexane extraction.
- Urea inclusion fractionation can reduce cloud point (CP) by over 20 ºC for biodiesels containing less than 20% saturated FAMEs.
- CP of palm oil FAMEs reached as low as -17 ºC after double urea inclusion fractionation.

GRAPHICAL ABSTRACT

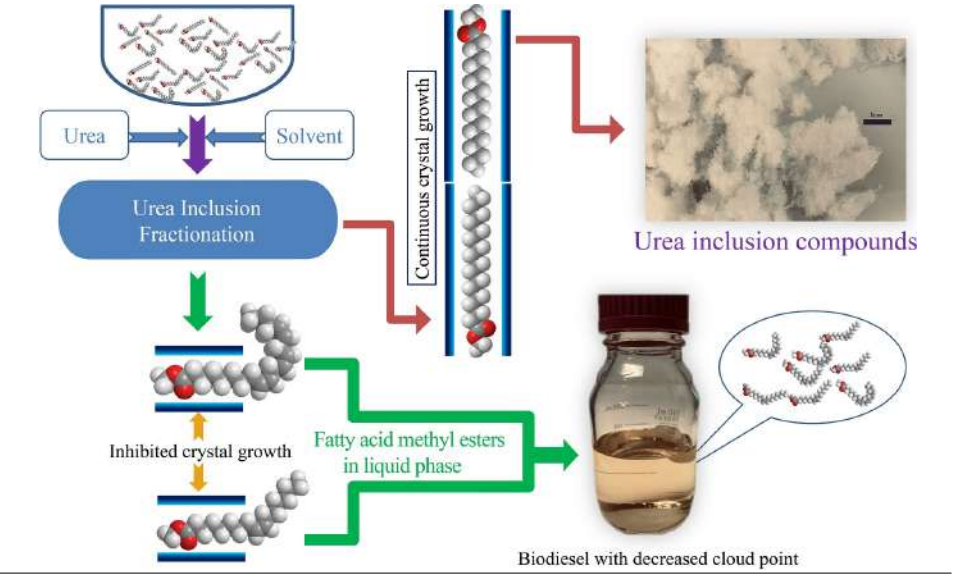

ARTICLE INFO

Article history:
Received 14 January 2022
Received in revised form 7 March 2022
Accepted 31 March 2022
Published 1 June 2022

Keywords:
Biodiesel
Fractionation
Cloud point
Cetane number
Oxidation stability
Emissions

ABSTRACT

Biodiesel is viewed as the alternative to petroleum diesel, but its poor low-temperature performance constrains its utilization. Cloud point (CP), the onset temperature of thermal crystallization, appropriately shows the low-temperature performance. The effective way to reduce CP is to remove saturated fatty acid methyl esters (FAMEs). Compared to current methods, this work describes an extraordinary approach to fractionating FAMEs by forming solid urea inclusion compounds (UICs). Urea inclusion fractionation reduces the CPs by removing high melting-point linear saturated FAME components. Urea inclusion fractionation in this study was performed under various processing conditions: mass ratios of urea to FAMEs and solvents to FAMEs, various solvents, FAMEs from various feedstocks, and processing temperatures. Supersaturation of urea in the solution is the driving force, and it significantly affects yield, composition, CP, separation efficiency, and selectivity. Through a single urea inclusion fractionation process, FAMEs, except palm oil FAMEs, resulted in CP reduction ranging from 20 to 42 ºC with a yield of 77–80% depending on the compositions. CP of palm oil FAMEs could reach as low as -17 ºC with a yield of 46% after twice urea inclusion fractionation. According to the model prediction, the cetane number after urea inclusion fractionation decreased about 0.7–2 but was still higher than the minimum biodiesel requirement. Oxidation stability after urea inclusion decreased according to the proposed model, but this can be mitigated by adding antioxidants. Emission evaluation after urea inclusion fractionation indicated decreased hydrocarbons, carbon monoxide, and particulate matter. However, it resulted in the increasing emission of nitrogen oxides.

* Corresponding author at: Tel.: +1 5188886988
E-mail address: liu18@purdue.edu

Please cite this article as: Liu J., Tao B. Fractionation of fatty acid methyl esters *via* urea inclusion and its application to improve the low-temperature performance of biodiesel. Biofuel Research Journal 34 (2022) 1617-1629. DOI: 10.18331/BRJ2022.9.2.3

Contents

Abbreviations

BMEP	Break mean effective pressure
CFPP	Cold filter plugging point
CN	Cetane number
CP	Cloud point
DU_m	Modified degree of unsaturation
FAMEs	Fatty acid methyl esters
FFAs	Free fatty acids
FID	Flame ionization detection
ID	Internal diameter
LTFT	Low-temperature flow test
L-FAMEs	FAMEs in liquid phase after urea inclusion fractionation
NR	Not reported
S-FAMEs	FAMEs in solid UICs after urea inclusion fractionation
PP	Pour point
SCSF	The straight-chain saturated factor
UIC	Urea inclusion compound

Nomenclatures

C16:0	Methyl palmitate
C16:1	Methyl palmitoleate
C18:0	Methyl stearate
C18:1	Methyl oleate
C18:2	Methyl linoleate
C18:3	Methyl linolenate
$C_{C=C}$	Carbon double bonds concentration
Cn:1	Methyl esters with 1 double bond and carbon chain length of n
Cn:2	Methyl esters with 2 double bonds and carbon chain length of n
Cn:3	Methyl esters with 3 double bonds and carbon chain length of n
$MW_{FAME,i}$	Molecule weight of i^{th} FAME
MW_U	Molecule weight of urea
$MW_{C18:1}$	Molecule weight of C18:1
$MW_{C18:2}$	Molecule weight of C18:2
$MW_{C18:3}$	Molecule weight of C18:3

Symbols

α	Ratio of initial weight of urea to initial weight of FAMEs
β	Ratio of initial weight of solvent to initial weight of FAMEs
m^0_{FAMEs}	Initial weight of FAMEs
$m^0_{FAME,i}$	Weight of i^{th} FAME in initial FAMEs
$m_{L\text{-}FAME,i}$	Weight of i^{th} FAME in L-FAMEs
$m_{S\text{-}FAME,i}$	Weight of i^{th} FAME in S-FAMEs
$m^0_{Solvent}$	Initial weight of solvent
m^0_U	Initial weight of urea
$m_{U/F,i}$	Mass ratio of urea to i^{th} FAME in UIC
$m_{U\text{-}L}$	Weight of urea in the saturated solution
m_{UIC}	Weight of UICs
$x_{C18:1}$	Weight percentage of C18:1
$x_{C18:2}$	Weight percentage of C18:2
$x_{C18:3}$	Weight percentage of C18:3
$x_{L-FAME,i}$	Weight percentage of i^{th} FAME in L-FAMEs
$x_{S-FAME,i}$	Weight percentage of i^{th} FAME in S-FAMEs
x^S_U	Solubility of urea in solution
x^0_U	Initial mass fraction of urea in the solution
T_m	Melting point
ε_i	Selectivity of i^{th} FAME in urea inclusion fractionation
σ	Driving force of urea inclusion fractionation
η_i	Separation efficiency of i^{th} FAME
γ_i	Stoichiometry of urea in urea inclusion fractionation

Please cite this article as: Liu J., Tao B. Fractionation of fatty acid methyl esters *via* urea inclusion and its application to improve the low-temperature performance of biodiesel. Biofuel Research Journal 34 (2022) 1617-1629. DOI: 10.18331/BRJ2022.9.2.3

1. Introduction

Elevated concerns about environmental problems associated with the widespread use of fossil fuels (Vohra et al., 2021; Thurston, 2022) have prompted intensive research on alternative renewable energy to meet the continuously growing demands. Biodiesel is viewed as the alternative to diesel fuels, which account for approximately 24% of transportation fuel and 21% of total crude oil consumption in the United States. Biodiesel conversion technology depends on feedstocks' free fatty acids (FFA) content. Transesterification with alcohols under catalytical conditions is a state-of-the-art method for FFA less than 2% in feedstocks (Sharma and Singh, 2009; Atabani et al., 2012). Otherwise, to inhibit the saponification, the esterification under acid catalytic conditions is carried out to convert FFA to fatty acid esters (Silitonga et al., 2014; Bai et al., 2022). Then, the transesterification is performed similarly to the low FFA feedstocks. The annual biodiesel production has been about 1.8 billion gallons since 2018 (Monthly Energy Review, 2022), and the primary feedstock is soybean oil, which accounts for over 60% of total feedstocks (Monthly Biodiesel Production Report, 2021). The other feedstocks include canola oil, corn oil, poultry, and tallows (Monthly Biodiesel Production Report, 2021). Methanol is the primary alcohol used in biodiesel production, and biodiesel comprises a mixture of fatty acid methyl esters (FAMEs) after the reactions. However, the FAMEs compositions are constrained by the source of oils/fats. The major FAMEs shown in **Figure 1** include methyl palmitate (C16:0), methyl palmitoleate (C16:1), methyl stearate (C18:0), methyl oleate (C18:1), methyl linoleate (C18:2), and methyl linolenate (C18:3). According to the melting points, FAMEs can be separated into high-melting-point and low-melting-point FAMEs. In addition, FAMEs can be divided into linear saturated FAMEs and nonlinear unsaturated FAMEs according to the molecular structure. Linear saturated FAMEs have high melting points, but nonlinear unsaturated FAMEs have low melting points. The variance in the composition of the FAMEs can significantly affect the biodiesel's qualities, such as low-temperature performance.

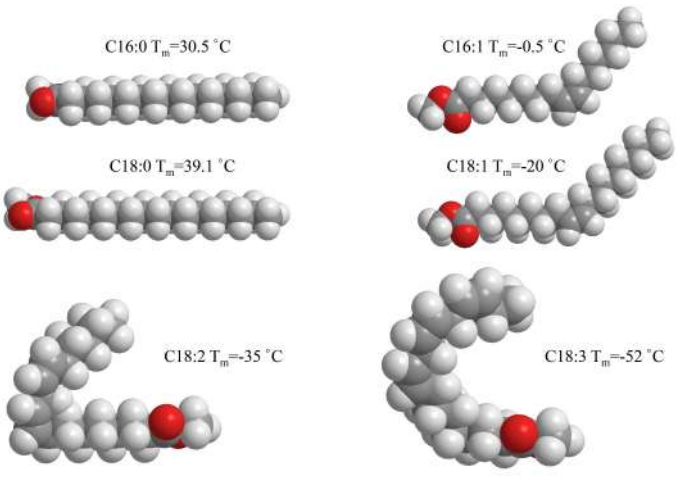

Fig. 1. Structures and the melting points of the major FAMEs in biodiesel (Foon et al., 2006; Sigma-Aldrich: http://www.sigmaaldrich.com/US/en/product/sigma/p9667).

Though biodiesel owns renewability and sustainability, its poor low-temperature performance constrains the utilization scopes. With the surrounding temperature decreasing, FAMEs with high-melting points tend to form solid crystals, and these crystals can block filters and lines. Four standards in ASTM D 6751 are used to evaluate the low-temperature performance: CP, pour point (PP), cold filter plugging point (CFPP), and low-temperature flow test (LTFT). **Table 1** shows the low-temperature performance of biodiesel produced from various feedstocks. CP appropriately describes the physical phase change concerning the temperature compared to other standards. CP of biodiesel ranges from -5 to 21 ºC for various feedstocks. Therefore, biodiesel generally has a higher CP than #2 diesel (-7 to -28 ºC) and #1 diesel (-40 ºC) (Nowatzki et al., 2019). Low-temperature performance needs to be improved to further promote biodiesel utilization.

Table 1.
Low-temperature performance of biodiesel from various feedstocks.

Biodiesel feedstock	Low-temperature performance				Ref .
	CP (ºC)	PP (ºC)	CFPP (ºC)	LTFT (ºC)	
Soy	3	-3	3	-2	Chiu et al. (2004); Tang et al. (2008)
Canola	-3	-4	-4	NR	McCormick (2006)
Corn	-3	-4	-7	NR	Dunn (2009)
Palm	15	12	9	NR	Boey et al. (2009)
Cotton seed	6	0	3	NR	Tang et al. (2008)
Rapeseed	0 to -3	-6 to -9	-4 to -9	NR	Rashid and Anwar (2008)
Sunflower	1.5	-3	-2	NR	Kalligeros et al. (2003)
Safflower	-5	-7.5	NR*	NR	Imahara et al. (2008)
Olive	-2	-3	-6	NR	Kalligeros et al. (2003)
Grease	8	6	1	NR	McCormick (2006)
Poultry fat	7	3	2	NR	Tang et al. (2008)
Tallow	17	15	9	20	Foglia et al. (1997)
Lard	13	13	11	NR	McCormick (2006)
Waste cooking oil	9	-3	NR	NR	Cetinkaya and Karaosmanoğlu (2004)
Jatropha curcas	20.2	18	NR	NR	Nainwal et al. (2015)

* NR: Not Reported.

Methods to improve the low-temperature performance of biodiesel can be classified as physical methods and chemical methods. There are two types of physical methods: mixing/blending and phase changing. The former includes adding crystallization inhibition additives and blending with petroleum diesel, ethanol, and butanol. Additives have a limited effect on the CP since they only can change the crystal growth habits (Shrestha et al., 2008; Senra et al., 2019). Blending with diesel and other alcohols results in reducing the usage of biodiesel. In addition, the CPs of the mixtures depend on the fractions and properties of diesel and alcohols (Lapuerta et al., 2018; Hazrat et al., 2020). The other physical methods based on phase change are thermal crystallization and distillation. Thermal crystallization is performed to remove the high-melting-point components by decreasing the surrounding temperature (González Gómez et al., 2002; Tajima et al., 2021). Also, it is an energy-intensive process with extending operation time to reach the equilibrium for the separation. Solvent extraction combined with thermal crystallization was applied to reduce CP with different solvents (Dunn et al., 1997), such as hexane and isopropanol. The disadvantages of this method are the high consumption of solvents, difficulty in process control from the surrounding temperature change, and CP reduction limitations even with decreasing operation temperatures. Another phase-changing method is biodiesel distillation fractionation (Su et al., 2011; Yeong et al., 2021). Besides high energy consumption, this operation is inhibited by the poor separation of the FAMEs with 18 carbon-chain in the fatty acid functional group because the difference in boiling points for these FAMEs is not significant. For all the phase change methods, saturated FAMEs are inevitable to residue in low CP portion due to phase equilibrium. As for the saturated FAMEs with high melting points, these methods have limited CP reduction. One chemical method is transesterification with longer carbon-chain alcohols (*vs* methanol), such as ethanol, propanol, butanol, and pentanol (Bouaid et al., 2014; Cardoso et al., 2014; Sierra-Cantor and Guerrero-Fajardo, 2017). This method reportedly decreases the CP by about 4 to 10 ºC but increases the production cost. Another chemical method is the alkoxylation of unsaturated components (Smith et al., 2009). However, this method increases CP in most cases. Hence, sometimes, two or more methods should be combined to reduce the CP.

Urea forms solid guest/host complexes with linear aliphatic compounds called urea inclusion compounds (UICs). This method has been used for fatty acid separation (Hayes et al., 1998; Wang et al., 2020). FAMEs and fatty acids have similar structures with different functional groups: ester *vs* carboxylic acid. Since C16:0 and C18:0 are linear molecules, they preferentially form UICs *vs* nonlinear C16:1, C18:1, C18:2, and C18:3 molecules (see **Fig. 1**). Therefore, urea inclusion fractionation can separate

Please cite this article as: Liu J., Tao B. Fractionation of fatty acid methyl esters *via* urea inclusion and its application to improve the low-temperature performance of biodiesel. Biofuel Research Journal 34 (2022) 1617-1629. DOI: 10.18331/BRJ2022.9.2.3

saturated/unsaturated FAMEs, and the FAMEs in liquid solution (L-FAMEs) become unsaturated enriched. The unsaturated enriched FAMEs result in significantly reduced CPs, suitable for cold weather fuels. Previous studies applied urea inclusion to fractionate biodiesel from corn oil (Bi et al., 2010) and soybean oil (Bist et al., 2009) to reduce the CP. However, these studies were only focused on specific biodiesel types. As the fatty acid profiles significantly vary in the different feedstocks, urea inclusion for various feedstocks needs to be studied. In addition, these studies focused on lowering CP as low as possible instead of providing a reference for the process. Unsaturated FAMEs are versatile chemicals that are viewed as biodiesel with good low-temperature performance as well as the feedstocks for polymers and bio-lubricants. Therefore, it is essential to minimize the unsaturated FAMEs lost. This paper applied urea inclusion fractionation to separate FAMEs from various sources, and the effects of the ratios of urea to solvent to FAMEs and operation temperatures on the separation efficiency were quantified. The feasibility of producing biodiesel with low-temperature performance comparable to winter season diesel or #1 diesel was also investigated. In addition, the effects of urea inclusion fractionation on cetane number, oxidation stability, and emissions were evaluated.

2. Materials and Methods

2.1. FAMEs production

The catalyst solution was prepared by adding 5 g of potassium hydroxide (ACS, Sigma-Aldrich) to 115 mL of methanol (>99.9%, Mallinckordt Baker Inc.). Five hundred mL of oil from various sources (soybean oil, canola oil, corn oil, safflower oil, palm oil, grape seed oil, and flaxseed oil, purchased from a local grocery store) was added into a 1-L jacketed reaction system (CG-1949-X-300, Chemglass USA). The reaction vessel was connected to a heating/cooling circulator (8110, PolyScience, USA) to control the reaction temperature. The mixing speed was controlled by an overhead motor with the digital controller (CG-2033, Chemglass, USA). Once the oil temperature reached 50 ºC, the catalyst solution was slowly added to the reactor within 30 min. Then, the mixture was heated to 65 ºC and continuously stirred at this temperature for 1 h to convert the oil to FAMEs. After the reaction, the reactor was heated to 75 ºC to evaporate the residual methanol with a vacuum quickly. The mixture was transferred to a separation funnel and settled for 24 h for glycerol/FAMEs separation. The bottom glycerol layer was drained after settling, while the residual top FAMEs layer needed further treatments. The FAMEs layer was washed with 200 mL of distilled water containing 3 mL of acetic acid in a separatory funnel, and the aqueous phase was drained after 1-h settling. Then, 200 mL of distilled water was poured into the funnel, and the aqueous layer was drained after setting for 1 h. This step was repeated until the water layer in the funnel became clear. Then, the dehydration of the hydrated FAMEs was performed in a rotary evaporator (BUCHI, Switzerland).

2.2. Urea inclusion process

The scheme of the urea inclusion process is shown in **Figure 2**. The solvents used in this study were methanol (>99.9%, Mallinckordt Baker Inc.), ethanol (>99.9%, Mallinckordt Baker Inc.), and n-propanol (>99%, Mallinckordt Baker Inc.). The weight of FAMEs was fixed at 50 g in all experiments. However, the weight of urea (>99%, Mallinckordt Baker Inc.) and solvents varied according to their mass ratios concerning FAMEs. FAMEs from vegetable oils were produced as shown in the previous section, but FAMEs from chicken fat and waste cooking oil were purchased from a local biodiesel company. The mass ratio of urea to FAMEs varied from 0 to 1, while the mass ratio of solvent to FAMEs varied from 3 to 5. The mixture of urea, FAMEs, and solvent in a 1-L flask was heated to form a homogenous solution with the maximum temperatures limited to 5 ºC less than the boiling points of the solvents to prevent evaporation. Then, the solution was cooled down to room temperature (about 20 ºC) or 0 ºC by using ice, and the resulting solid/liquid mixture was separated by filtration. Two hundred mL hexane was used to rinse the UICs to minimize the L-FAMEs yield loss.

The solvent in the liquid filtrate was removed by a rotary evaporator (BUCHI, Switzerland). The residual was placed into a separatory funnel, and 200 mL of distilled water was added with mixing to remove residual urea and solvent, followed by removal of the water layer after 0.5-h settling. This step was repeated several times until the water layer became clear. The bottom layer was drained, and the top layer was put into a rotary evaporator (BUCHI, Switzerland) to remove the moisture to obtain L-FAMEs. The solid residual in the filtration was mixed with hot water to decompose the UICs. Then, the mixture was transferred to a separation funnel, and 150 mL of hexane was added to maximize the recovery of the FAMEs. The hexane was recovered in a rotary evaporator after the hexane layer was transferred, and the residual liquid was the FAMEs in solid UICs after urea inclusion fractionation (S-FAMEs). The compositions of L-FAMEs and S-FAMEs were analyzed according to the method mentioned in the following section.

2.3. Urea solubility in alcohols

Urea solubility in alcohols was measured at 0 and 20 ºC. Two hundred g of alcohol was put into a 500 mL flask, and about 60 g of urea was added to the solution. The capped flask was placed in a heating/cooling circulator (Polyscience 9702, Polyscience, USA) at the given temperature for 24 h. A certain amount of liquid solution was moved to another flask and weighed. The alcohol was evaporated by a rotary evaporator (BUCHI, Switzerland), and the residual urea was measured. Urea solubility was determined by the ratios of residual urea weight to the solution's weight.

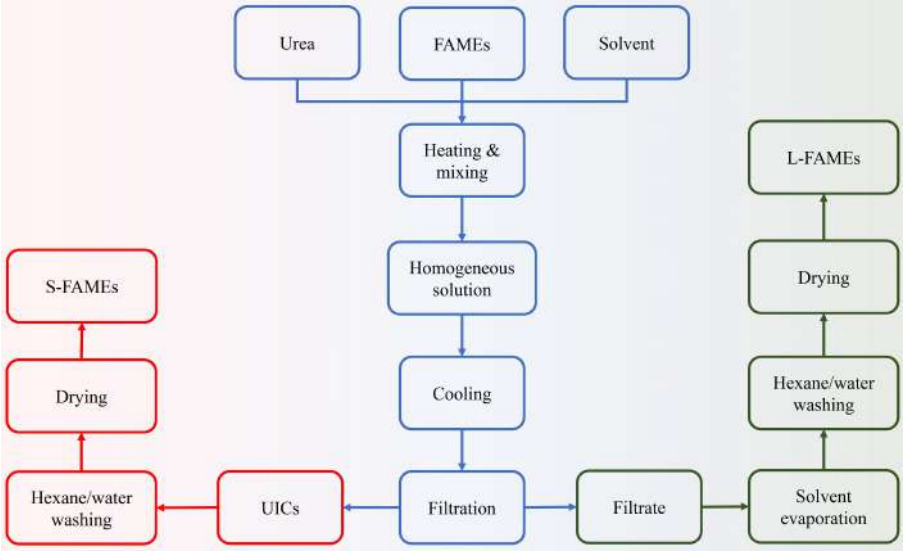

Fig. 2. Scheme of the cooling urea inclusion process.

Please cite this article as: Liu J., Tao B. Fractionation of fatty acid methyl esters *via* urea inclusion and its application to improve the low-temperature performance of biodiesel. Biofuel Research Journal 34 (2022) 1617-1629. DOI: 10.18331/BRJ2022.9.2.3

2.4. CP measurement

For measuring CP values in the range of 20 to -40 ºC, a CPA-T30 cloud point analyzer (Phase Technology, Richmond, Canada) was used. For CP values less than -40 ºC, CP was measured according to the ASTM D 2500. For the samples tested by ASTM D 2500, dry ice with ethanol was used to control the bath temperature, and a 5 mL sample in a 100 mL glass tube was placed in a stainless-steel cylinder. The stainless-steel cylinder was dipped into the bath to chill the sample. The temperature (i.e., CP temperature) was recorded when the first crystal was visually observed.

2.5. Composition analysis

The composition of FAMEs was determined by gas chromatography (GC Trace Ultra, Thermo Scientific Inc., Milan, Italy) using an RTX-5 column (7 M×0.32 mm ID) and flame ionization detection (FID). The column temperature was increased to 220 ºC at 30 ºC/min after being kept at 130 ºC for 0.5 min. Then, the column temperature ramped up to 250 ºC at 10 ºC/min after being held at 220 ºC for 1 min. The column temperature was maintained at 250 ºC for 4 min. Both the injection temperature and FID temperature were 250 ºC.

3. Results and Discussion

3.1. Effects of mass ratios of urea to FAMEs on urea inclusion fractionation

Urea is the crucial component in urea inclusion as it forms the hexagonal host structure around the guest molecules. UIC formation depends on the supersaturation in the solutions, and the supersaturation can be achieved by lowering the solution temperature. The mass ratio of the initial amount of urea to the initial amount of FAMEs is defined as α (**Eq. 1**).

$$\alpha = m_U^0 / m_{FAMEs}^0 \quad \text{Eq. 1}$$

where α is the ratio of the initial weight of urea to the initial weight of FAMEs, m_U^0 the initial weight of urea, and m_{FAMEs}^0 the initial weight of FAMEs.

For α less than 0.2, no UICs were formed because urea was not supersaturated in the solution. Therefore, the FAMEs compositions did not change (**Fig. 3a**). For α greater than 0.4, urea became supersaturated in the solution to form UICs, and the fractions of solid UICs increased with α (**Fig. 3b**). Moreover, α significantly changed the compositions of L-FAMEs and S-FAMEs (**Fig. 3**). Generally, linear saturated FAMEs, C18:0 and C16:0, decreased in L-FAMEs with α, while nonlinear polyunsaturated FAMEs, C18:2 and C18:3, increased in L-FAMEs with α. However, the nonlinear monounsaturated FAME, C18:1, slightly increased to the maximum for α at 0.8, but then it started to decrease. The particular change of C18:1 resulted from the significant decrease in linear saturated FAMEs and the relatively high linearity of C18:1 compared to polyunsaturated FAMEs. C18:0 in S-FAMEs continuously decreased with α, while C16:0 had the maximum for α at 0.8. Meanwhile, the unsaturated FAMEs kept approximately constant before increasing to α above 0.8. This phenomenon indicated that C18:1 became the main FAME in UICs when insignificant or no saturated FAMEs existed in FAMEs.

The capability of urea inclusion fractionation in removing FAMEs to form UICs increased with the mass ratios of urea to FAMEs (**Fig. 4a**). The preference for moving components from liquid solutions to solid UICs follows the order: C18:0 > C16:0 > C18:1 > C18:2 > C18:3. A similar trend was reported in a previous report (Bi et al., 2010). The crystals can continue to grow for linear components, but crystal growth is inhibited by the bent structures caused by the carbon double bonds (**Fig. 1**). Separation efficiency, defined in **Equation 2**, was applied to quantify the preference of various FAMEs to form UICs in urea inclusion fractionation. With the saturated FAMEs being fractionated out from the solution, CPs of the residual L-FAMEs decreased with the mass ratios of urea to FAMEs (**Fig. 4a**).

The driving force of urea inclusion fractionation is the supersaturation of urea under given conditions. The solubility of urea in methanol/FAMEs was quantified as the mass fraction of urea in the liquid phase after urea inclusion fractionation in **Equation 3**. The driving force was quantified as the difference between the initial urea mass fraction in solution and the final urea solubility

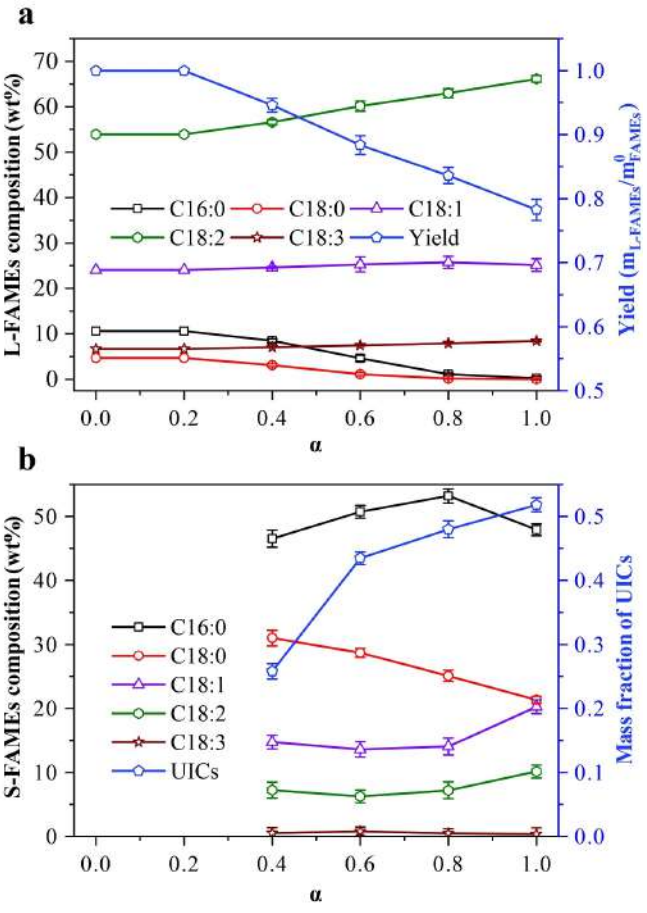

Fig. 3. Effect of mass ratio of urea to FAMEs (α) on the compositions of FAMEs in the liquid phase (L-FAMEs) and FAMEs in UICs (S-FAMEs) (wt%), yields of L-FAMEs, and UIC fraction under the processing conditions of soy FAMEs (50 g), urea (0, 10, 20, 30, 40, and 50 g), methanol (200 g), and UIC formation temperature (0 ºC); **(a)** compositions and yields of L-FAMEs and **(b)** compositions of S-FAMEs and mass fraction of UICs.

in the liquid solutions (**Eq. 4**). According to **Figure 4b**, the solubility of urea in methanol/FAMEs is less than that in pure methanol. The solubility of urea (mass fraction) in pure methanol at temperatures close to 0 ºC is 0.071 (Lee and Lahti, 1972). Moreover, the solubility in the methanol/FAMEs solution was affected by the compositions of FAMEs. The solubility of urea in methanol/FAMEs solution increased as the saturated FAMEs fractions decreased. The driving force was linearly increased with the mass ratios of urea to FAMEs (**Eq. 5**).

With driving forces increasing, urea fractionation preferred the saturated FAMEs to the unsaturated FAMEs to be transferred to solid UICs. Consequently, the CPs of L-FAMEs decreased. The driving force quantified the urea fractionation process as the solid-liquid phase equilibrium. Furthermore, according to a previous report (Bi et al., 2010), the equilibrium could be viewed as a fast process, as the time had less effect on the final composition.

$$\eta_i = m_{L-FAME,i} / m_{FAME,i}^0 \quad \text{Eq. 2}$$

$$x_U^S = m_{U\text{-}L} / \left(m_{Solvent}^0 + m_{L\text{-}FAMEs} + m_{U\text{-}L} \right) \quad \text{Eq. 3}$$

$$\sigma = m_U^0 / \left(m_{Solvent}^0 + m_{FAMEs}^0 + m_U^0 \right) - x_U^S \quad \text{Eq. 4}$$

Please cite this article as: Liu J., Tao B. Fractionation of fatty acid methyl esters *via* urea inclusion and its application to improve the low-temperature performance of biodiesel. Biofuel Research Journal 34 (2022) 1617-1629. DOI: 10.18331/BRJ2022.9.2.3

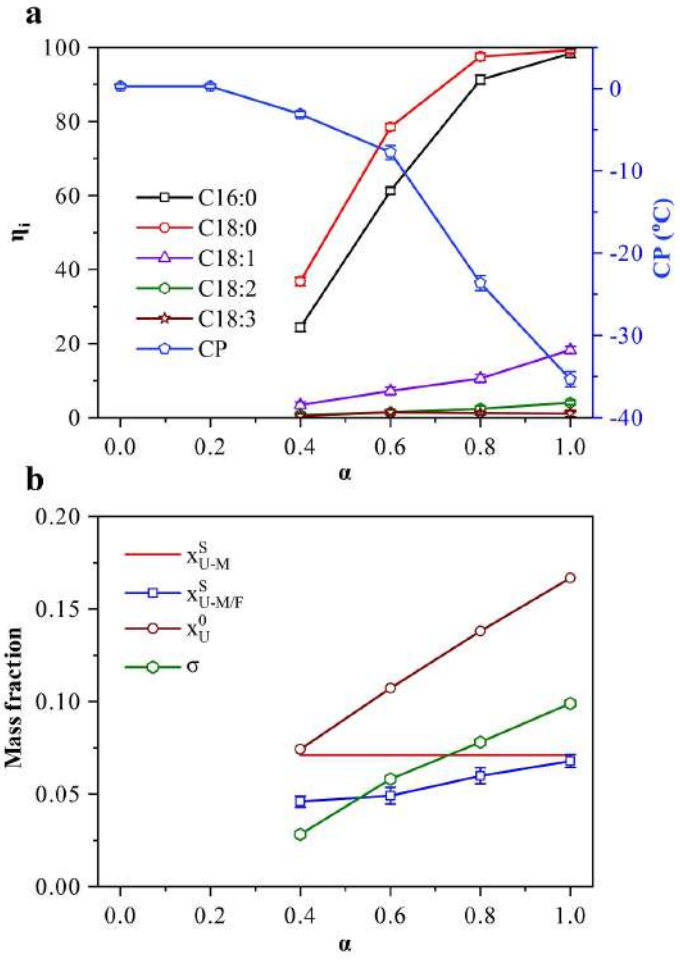

Fig. 4. Effect of mass ratio of urea to FAMEs (α) on the separation efficiency (ηi), CP, and driving force (σ) for urea inclusion fractionation under the processing conditions of soy FAMEs (50 g), urea (0, 10, 20, 30, 40, and 50 g), methanol (200 g), and UIC formation temperature (0 °C); **(a)** separation efficiency and CP, and **(b)** driving force analysis. x^0_U: initial mass fraction of urea in the solution; x^S_{U-M}: solubility of urea in methanol; and $x^S_{U-F/M}$: solubility of urea in methanol/urea/FAMEs mixture.

$$\sigma = 0.116 \times \alpha - 0.015 \qquad R^2 = 0.985 \qquad \text{Eq. 5}$$

where η_i is the separation efficiency of ith FAME, $m_{L\text{-}FAME,i}$ the weight of ith FAME in L-FAMEs, $m^0_{FAME,i}$ the weight of ith FAME in initial FAMEs, x^S_U the solubility of urea in solution, $m_{U\text{-}L}$ the weight of urea in the saturated solution, $m^0_{Solvent}$ the initial weight of solvent, and σ the driving force of urea inclusion fractionation.

3.2. Effect of solvents on urea inclusion fractionation

Urea inclusion fractionation depends on the urea supersaturation in the solution. Besides ratios of urea to FAMEs, the ratios of solvents and various types of solvents also altered the supersaturation by changing the solubility of urea in FAMEs/solvent mixtures. First, methanol was used as the solvent to dissolve the urea and FAMEs in urea inclusion, and the amount of methanol changed the solubility of urea in the solution with a fixed amount of urea and FAMEs. β is defined as the ratio of the initial weight of urea to the initial weight of solvent (**Eq. 6**). **Figures 5** and **6** show that β could alter the urea inclusion fractionation by changing the solubility of urea in methanol/FAMEs solution. The driving force decreased with methanol increasing, which resulted in the decreasing capability to remove FAMEs, predominantly linear saturated FAMEs, from the liquid solution to solid UICs. Therefore, the yield and the saturated FAMEs increased with the ratios of methanol to FAMEs, but the separation efficiency decreased. Besides separation efficiency, UIC formation

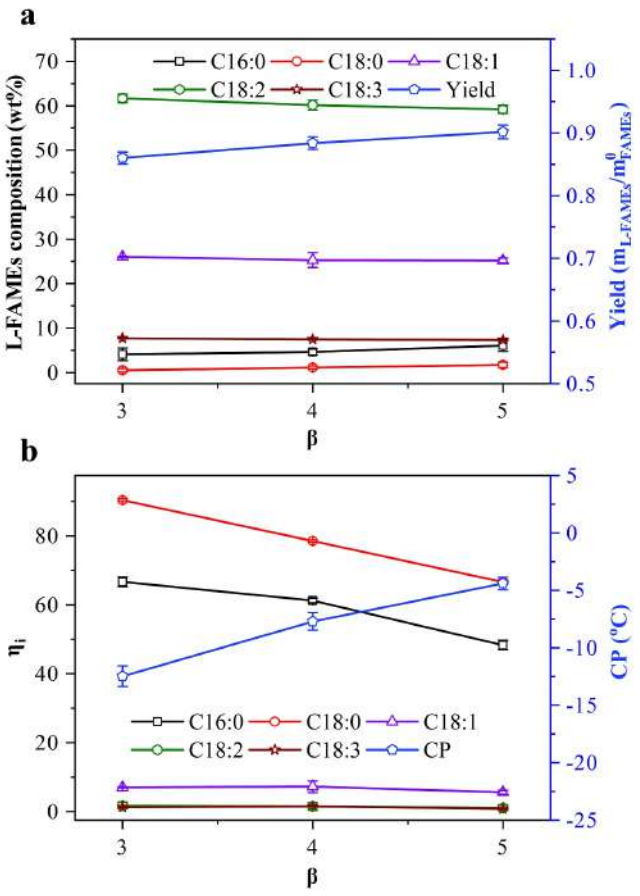

Fig. 5. Effect of mass ratio of methanol to FAMEs (β) on the composition of FAMEs in the liquid phase (L-FAMEs), separation efficiency (ηi), yield, and CP under the processing conditions of soy FAMEs (50 g), urea (30 g), methanol (150, 200, and 250 g), UIC formation temperature (0 °C) and various mass ratios of methanol to FAMEs; **(a)** composition and yield of L-FAMEs, and **(b)** separation efficiency and CP.

preference can also characterize urea inclusion's selectivity, as shown in **Equation 7**. The components preferred forming solid UICs for formation preference less than 1, such as C16:0 and C18:0. However, the components favored retaining in the liquid phase for the preference above 1. With the saturated FAMEs in L-FAMEs decreasing, CP decreased with the ratio of methanol to FAMEs. However, there was a minimum amount of solvent for the given amounts of urea and FAMEs. This research proved that no UICs could be formed without solvent in the solution because the amount of FAMEs did not change after the process. In addition, the existence of the minimum amount of solvent indicated that the crystal urea that did not dissolve in the solvent could not form UICs with host molecules. It was also proved by a previous study that yield and composition did not change when the amount of solvent was less than a certain level (Bi et al., 2010). This study revealed that the minimum β for α at 0.6 and 1 were 3 and 4, respectively.

$$\beta = m^0_{Solvent} / m^0_U \qquad \text{Eq. 6}$$

where β is the ratio of the initial weight of solvent to the initial weight of FAMEs.

$$\varepsilon_i = x_{L-FAME,i} / x_{S-FAME,i} \qquad \text{Eq. 7}$$

where ε_i is the selectivity of ith FAME in urea inclusion fractionation, $x_{L-FAME,i}$ the weight percentage of ith FAME in L-FAMEs, and $x_{S-FAME,i}$ the weight percentage of ith FAME in S-FAMEs.

Please cite this article as: Liu J., Tao B. Fractionation of fatty acid methyl esters *via* urea inclusion and its application to improve the low-temperature performance of biodiesel. Biofuel Research Journal 34 (2022) 1617-1629. DOI: 10.18331/BRJ2022.9.2.3

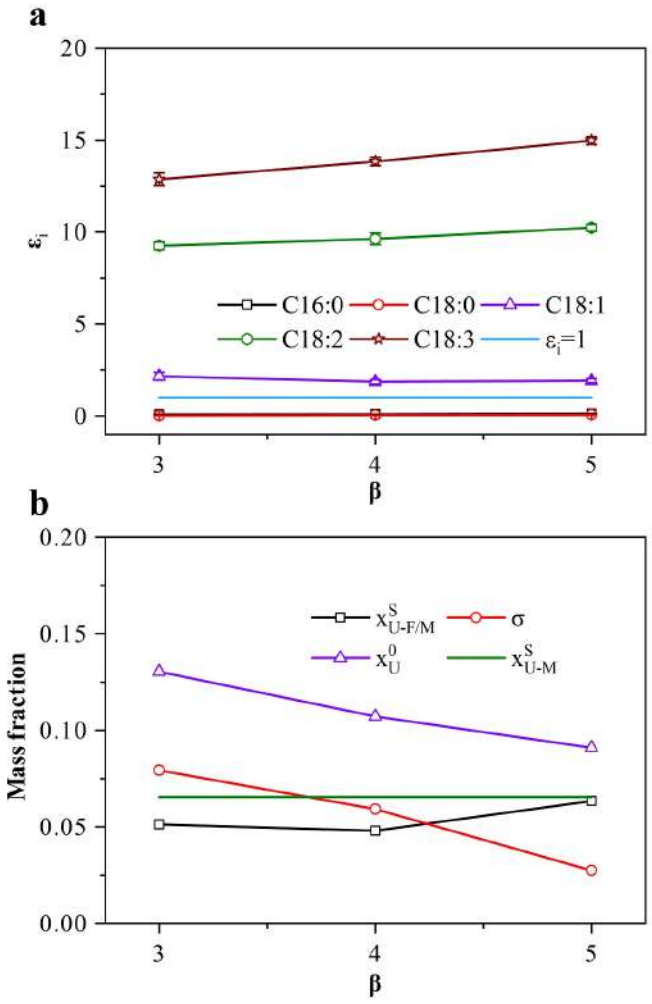

Fig. 6. Effect of mass ratio of methanol to FAMEs (β) on UIC formation preference and driving force (σ) under the processing conditions of soy FAMEs (50 g), urea (30 g), methanol (150, 200, and 250 g), UIC formation temperature (0 °C) **(a)** UIC formation analysis and **(b)** driving force analysis. εi: selectivity of ith FAME in urea inclusion fractionation; x_U^0: initial mass fraction of urea in the solution; x_{U-M}^S: solubility of urea in methanol; and $x_{U-F/M}^S$: solubility of urea in methanol/urea/FAMEs mixture.

The driving force can be altered by changing the amount of solvent in the solution, as discussed in the previous section. Another way to alter the driving force based on the solvents is to perform urea inclusion fractionation under different solvents. Methanol, ethanol, and n-propanol were used in urea inclusion fractionation with the same mass ratios of urea to FAME to solvent, as shown in Figures 7 and 8. Urea solubility in pure solvents follows methanol > ethanol > n-propanol. The carbon chain length in solvents differs for various alcohols: 1 referred to methanol; 2 referred to ethanol; 3 referred to n-propanol. With FAMEs added to the solution, the solubility decreased, and the driving force increased with the carbon chain length. Therefore, the yield of L-FAMEs decreased with solvent carbon chain length. With the increasing solvent carbon chain length, the percentage of polyunsaturated FAMEs increased while the percentage of saturated and monounsaturated FAMEs decreased. Because most saturated FAMEs were fractionated out from the solution, monounsaturated FAME became the main component in UIC formation. This phenomenon could be informed by the UICs formation preference being close to 1. With the saturated FAMEs moving to solid UICs, CP decreased with increased solvent carbon chain length. Compared to the changing ratio of methanol to FAMEs, urea inclusion with a long carbon chain solvent could result in better separation. However, the urea level (mass ratio of urea to FAMEs in 1-propanol was limited to 0.6) was limited, and it required a higher heating temperature to make a homogenous solution for urea inclusion. Consequently, the processing amount could be inhibited, and the energy consumption could increase.

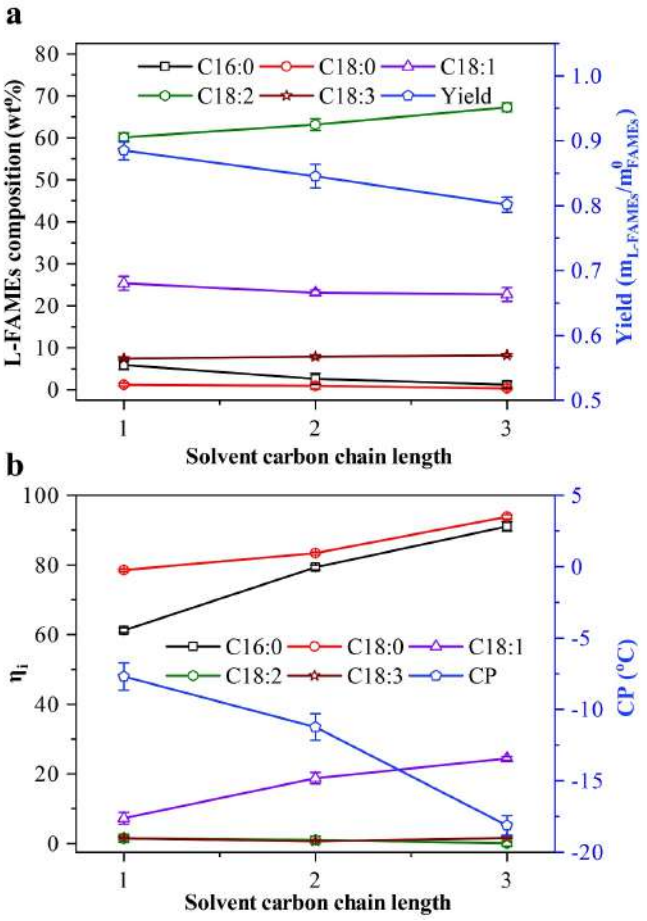

Fig. 7. Compositions, yields, and CPs of L-FAMEs and separation efficiency (η_i) of urea inclusion fractionation with various solvents (1: methanol; 2: ethanol; 3: n-propanol) under the operation conditions of soy FAMEs (50 g), urea (30 g), solvent (200 g), and UIC formation temperature (0 °C) **(a)** composition and yield of L-FAMEs, and **(b)** separation efficiency and CPs.

3.3. Effect of operation temperature

The urea inclusion temperature also changes the driving force by changing the urea solubility. Compared to operation at 0 °C, Figure 9 shows the changes in compositions, solubility, and driving force for operation temperature at 20 °C. Saturated FAMEs in L-FAMEs increased with temperature, but unsaturated FAMEs in FAMEs decreased with temperature. The changing behavior resulting from the solubility of urea in the FAMEs/methanol mixture increased with temperature. With the existence of FAME, the solubility of urea decreased compared to pure methanol. For the given conditions, the driving force decreased as the solubility increased. Consequently, the capability to remove the FAMEs, particularly the saturated FAMEs, was reduced. Meanwhile, the yield and CP increased with temperature.

3.4. Effect of FAMEs from various sources

Biodiesel is mainly produced from soybean oil in the United States, but there are other feedstocks for biodiesel production, such as animal fats, canola oil, corn oil, palm oil, and waste cooking oil. So, the feasibility of urea inclusion fractionation for these feedstocks should also be determined. In order to enlarge the utilization scope, some feedstocks with particular fatty acid profiles were also used in the present work, such as flaxseed oil with high C18:3, safflower oil with high C18:1 and minor C18:3, and grapeseed oil and sunflower oil with high C18:2 and minor C18:3. Figure 10 presents the composition changes after urea inclusion fractionation. Through urea inclusion fractionation, saturated FAMEs significantly

Please cite this article as: Liu J., Tao B. Fractionation of fatty acid methyl esters *via* urea inclusion and its application to improve the low-temperature performance of biodiesel. Biofuel Research Journal 34 (2022) 1617-1629. DOI: 10.18331/BRJ2022.9.2.3

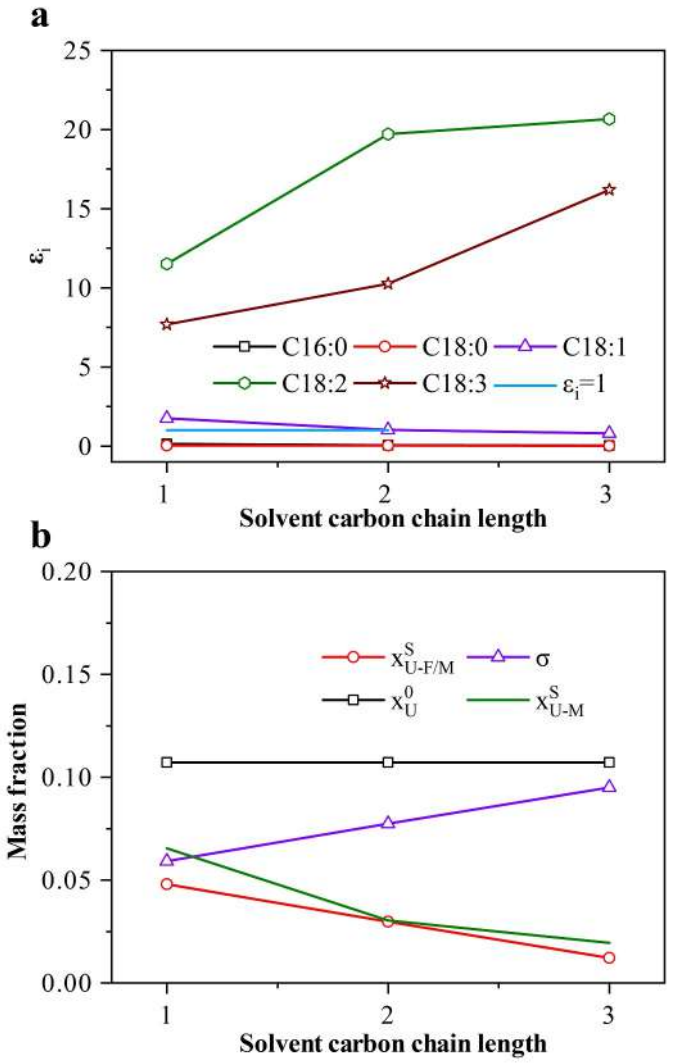

Fig. 8. Effect of solvent type (1: methanol; 2: ethanol; 3: n-propanol) on UIC formation preference and driving force (σ) under the processing conditions of soy FAMEs (50 g), urea (30 g), solvent (200 g), UIC formation temperature (0 °C); **(a)** UIC formation analysis and **(b)** driving force analysis. εi: selectivity of ith FAME in urea inclusion fractionation; x_U^0: initial mass fraction of urea in the solution; x_{U-M}^S: solubility of urea in methanol; and $x_{U-F/M}^S$: solubility of urea in methanol/urea/FAMEs mixture.

decreased with the driving force of urea supersaturation. Meanwhile, the polyunsaturated FAMEs were enriched in L-FAMEs.

For saturated FAMEs percentages less than 20%, nearly all saturated FAMEs were fractionated out from L-FAMEs and CP was significantly reduced. For the same operation conditions, the yield of L-FAMEs varied, resulting from the FAMEs composition. High saturated FAMEs feedstocks had a lower yield. A pseudo physical reaction mechanism is proposed in **Equation 8** to infer the variance in yield for various feedstocks. The mass ratio of urea to FAME in UICs could be calculated from the mechanism presented in **Equation 9**. The stoichiometry coefficients of urea, the number of urea molecules per ith type of FAME molecule, γ_i, could show the required amount of urea to move ith type of FAME out from the solution to form UICs. Therefore, linear regression of multi variables was performed to obtain the γ_i according to **Equation 10**, and γ_i for various FAME is shown in **Table 2**. Generally, the mass ratio of urea to FAMEs in UICs is about 3 for saturated FAMEs. However, the mass ratio of urea to FAMEs in UICs is less than 3. FAMEs with high saturated FAMEs (such as palm oil FAMEs) had a high driving force and resulted in less urea in the solution for the same operating conditions. Therefore, more FAMEs were transported to solid UICs, resulting in a lower yield of L-FAMEs (**Fig. 11a**). However, FAMEs with low saturated FAMEs

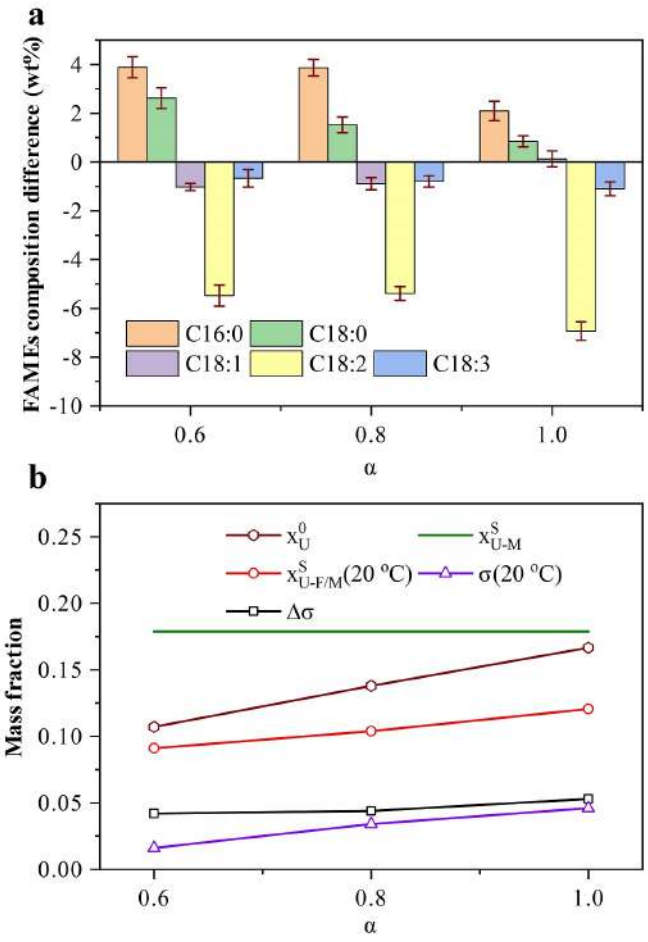

Fig. 9. Changes in FAMEs composition, driving force (σ), and solubility under various operation temperatures (0 and 20 °C) with the process conditions: soy FAMEs (50 g), urea (30, 40, and 50 g), and methanol (200g); **(a)** composition change and **(b)** driving force analysis and driving force change. α: mass ratios of urea to FAMEs; x_U^0: initial mass fraction of urea in the solution; x_{U-M}^S: solubility of urea in methanol; $x_{U-F/M}^S$(20 °C): solubility of urea in methanol/urea/FAMEs mixture at 20 °C; σ(20 °C): urea inclusion fractionation driving force at 20 °C; Δσ: driving force difference between operation at 20 and 0 °C.

Table 2.
Molar ratio and mass ratio of urea to FAME in UICs.

	Experimental regression		Ref. (Schlenk, 1954)	
	γi	mU/F,i	γi	mU/F,i
C16:0	13.821±0.804	3.069±0.178	13.5	2.997
C18:0	15.001±1.581	3.018±0.318	14.8	2.978
C18;1	14.610±0.193	2.960±0.039	14.5	2.937
C18:2	13.478±1.284	2.749±0.262	14.2	2.896
C18:3	12.341±1.476	2.534±0.303	13.7	2.813

(such as flaxseed oil FAMEs) had a lower driving force, and more urea was left in the liquid phase. Consequently, urea inclusion fractionation of these types of FAMEs resulted in a less yield of L-FAMEs. According to previous studies (Bi et al., 2010; Lee et al., 2014), the significant yield loss of L-FAMEs could result from hot water wash. This work minimized the yield loss by using hexane to rinse the UICs.

$$\gamma_i U + FAME_i \; f \;\; \gamma_i U \cdot FAME_i \qquad \text{Eq. 8}$$

$$m_{U/F,i} = \gamma_i MW_U \,/\, MW_{FAME,i} \qquad \text{Eq. 9}$$

Please cite this article as: Liu J., Tao B. Fractionation of fatty acid methyl esters *via* urea inclusion and its application to improve the low-temperature performance of biodiesel. Biofuel Research Journal 34 (2022) 1617-1629. DOI: 10.18331/BRJ2022.9.2.3

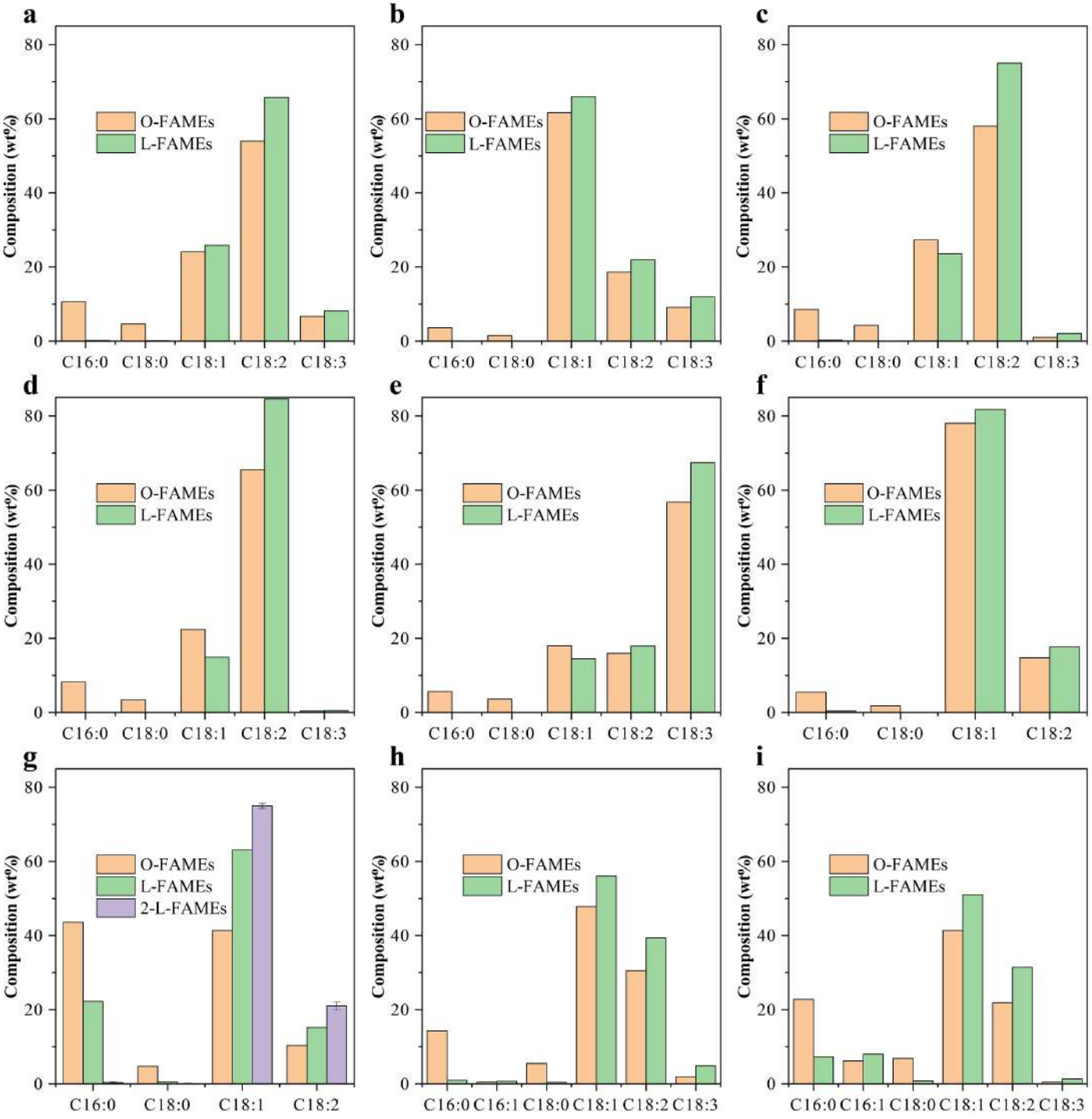

Fig. 10. Comparison of the original FAMEs (O-FAMEs) composition to L-FAMEs after urea inclusion fractionation under the following operation conditions: FAMEs (50 g), urea (50 g), methanol (200 g), and operating temperature of 0 °C; **(a)** soybean oil FAMEs, **(b)** canola oil FAMEs, **(c)** corn oil FAMEs, **(d)** grape oil FAMEs, **(e)** flaxseed oil FAMEs, **(f)** high oleic safflower oil FAMEs, **(g)** palm oil FAMEs, **(h)** waste cooking oil FAMEs, and **(i)** chicken fat FAMEs.

$$\gamma_i MW_U \left(m^0_{FAME,i} x^0_{FAME,i} - m^0_{L-FAME,i} x^0_{L-FAME,i} \right) \Big/ MW_{FAME,i} = m^0_U - m_{U-L} \quad \text{Eq. 10}$$

where γ_i is the stoichiometry of urea in urea inclusion fractionation, $m_{U/F,i}$ the mass ratio of urea to i[th] FAME in UIC, MW_U the molecule weight of urea, $MW_{FAME,i}$ the molecule weight of i[th] FAME, and m_{U-L} the weight of urea in the saturated solution.

After single urea inclusion fractionation (operation conditions: mass ratio of urea to FAMEs to methanol at 1:1:4 and operation temperature at 0 °C), CP of L-FAMEs, except palm oil biodiesel, was generally lower than

Please cite this article as: Liu J., Tao B. Fractionation of fatty acid methyl esters *via* urea inclusion and its application to improve the low-temperature performance of biodiesel. Biofuel Research Journal 34 (2022) 1617-1629. DOI: 10.18331/BRJ2022.9.2.3

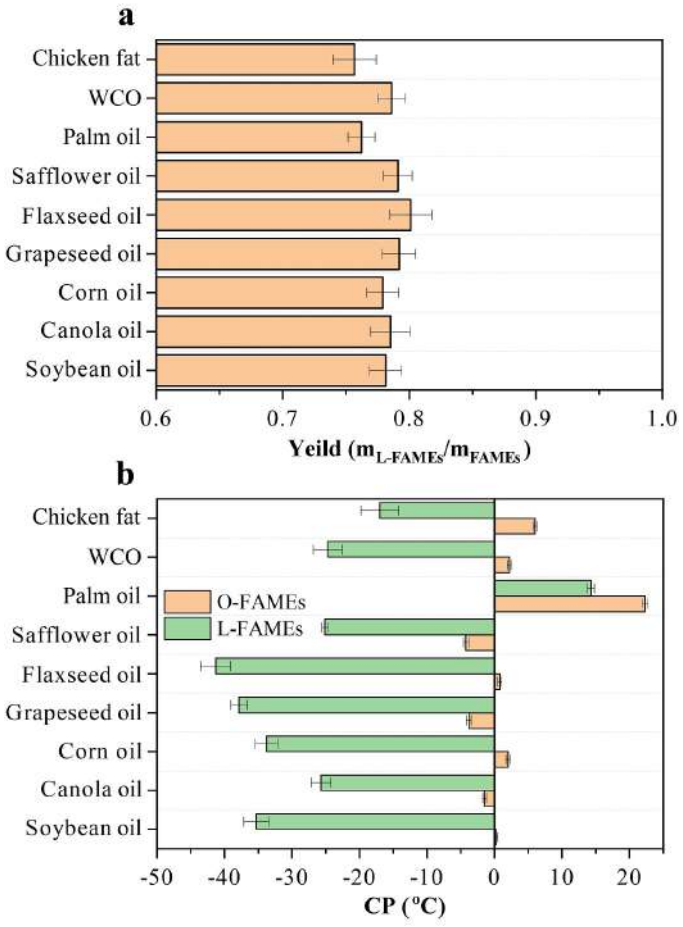

Fig. 11. Effect of urea inclusion fractionation on FAMEs from various feedstocks under the processing conditions of FAMEs (50 g), urea (50 g), methanol (200 g), and operating temperature of 0 °C. **(a)** yield of L-FAMEs and **(b)** CPs of original FAMEs (O-FAMEs) and L-FAMEs produced from different oil/fat feedstocks.

-18 °C (Fig. 11b), meeting the low-temperature performance requirement for winter season #2 diesel. In the case of palm oil biodiesel, the main saturated FAMEs could be removed after it underwent double times of urea inclusion. Then, after second urea inclusion, the CP of L-FAMEs could reach -17 °C, and the yield was about 46%.

3.5. Comparison with the other fractionation technologies

The application of the blending method for improving biodiesel's low-temperature performance possesses a major disadvantage, i.e., dependency of the blend's properties on the blended materials (diesel fuel, ethanol, butanol, etc.). On the other hand, additives have a limited effect on low-temperature performance at low dosages. These methods are not favorable because of increasing the production cost while offering little improvements in low-temperature performance. Therefore, only the fractionation technologies are compared herein, i.e., distillation, winterization, and urea inclusion fractionation. As shown in Table 3, urea inclusion fractionation offers the fastest production rate and high yields. In addition, urea inclusion was more flexible in operation as the urea amount could be changed to meet the requirements. In addition, multiple urea inclusion fractionations could be applied to ultra-high saturated FAMEs to produce FAMEs with good low-temperature performance. Due to the equilibrium controlling distillation and winterization, the saturated FAMEs cannot be entirely removed from the mixtures. Therefore, the reduction extent of CP using these technologies is limited.

Table 3.
Comparison of various fractionation technologies.

Feedstock	Fractionation Technology	Initial CP (°C)	Obtained CP (°C)	Yield (%)	Operation time (h)	Ref.
Palm oil	Distillation	20	13	~40	1.6	Yeong et al. (2021)
	Winterization	18	12	~50	6 to 24	Yovany Benavides et al. (2008)
	Urea inclusion fractionation	23	14	~78	1 to 2	This work
	Double urea inclusion fractionation	23	-17	~46	2 to 4	This work
Waste cooking oil	Winterization	14.5	11.5	87.4		Nainwal et al. (2015)
	Winterization	2	-2 to 0	~30	8 to 19	González Gómez et al. (2002)
	Urea inclusion fractionation	2.2	-24	80	1	This work
Soybean oil	Winterization	3.7	-7.1	85	16	Lee et al. (1996)
	Winterization	0	-20	30 to 33	>3	Dunn et al. (1997)
	Solvent extraction	0.3	-8.7 to -11.3	59.6 to 86	>3	Dunn (2011)
	Urea inclusion fractionation	0.5	-18 to -35	78 to 83	1 to 2	This work
Corn oil	Urea inclusion fractionation	2	-33.8	78	1 to 2	This work
	Urea inclusion fractionation	-	-45	35 to 40	12	Bi et al. (2010)

3.6. Effect of changes in FAMEs composition on the other critical biodiesel specifications

In addition to CP, other biodiesel specifications significantly depend on the FAMEs composition, such as cetane number and oxidation stability. Cetane number indicates the combustion speed and compression need of biodiesel for ignition in the diesel engine. According to ASTM D 6751, the minimum cetane number for biodiesel is 47. Generally, saturated FAMEs have a higher cetane number, and the cetane number decreases with the carbon double bonds. According to a previous model used for predicting cetane number based on the FAMEs composition shown in **Equations 11-13** (Mishra et al., 2016), the cetane number after urea fractionation slightly decreased (**Fig. 12a**). However, the cetane number could still meet the minimum requirements for biodiesel.

$$CN=63.41-0.0728\times DU_m+0.03495\times SCSF-2.26\times10^{-4}\times DUm\times SCSF \quad \text{Eq. 11}$$

$$SCSF=\sum\left(MW_{FAME,i}\times wt\%\text{ of saturated FAMEs}\right)/100 \quad \text{Eq. 12}$$

$$DU_m=\left(\text{monounsaturated Cn:1, wt\%}\right)+2\times\left(\text{polyunsaturated Cn:2, wt\%}\right)+3\times\left(\text{polyunsaturated Cn:3, wt\%}\right) \quad \text{Eq. 13}$$

Please cite this article as: Liu J., Tao B. Fractionation of fatty acid methyl esters *via* urea inclusion and its application to improve the low-temperature performance of biodiesel. Biofuel Research Journal 34 (2022) 1617-1629. DOI: 10.18331/BRJ2022.9.2.3

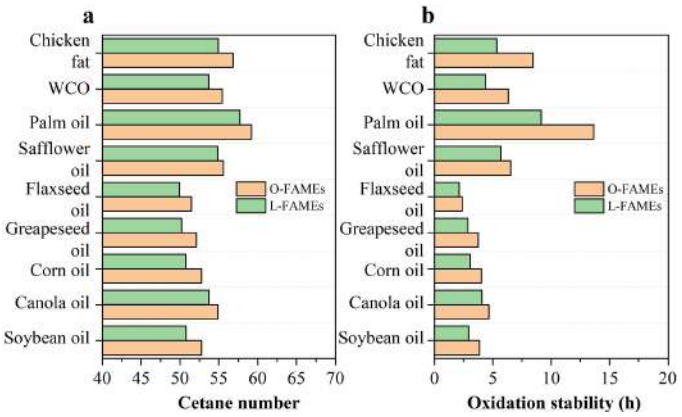

Fig. 12. Changes in cetane number and oxidation stability after urea inclusion fractionation under the operation conditions: FAMEs (50 g), urea (50 g), methanol (200 g), and operating temperature of 0 °C. **(a)** cetane number and **(b)** oxidation stability of original FAMEs (O-FAMEs) and L-FAMEs produced from different oil/fat feedstocks.

where CN is cetane number, SCSF the straight-chain saturated factor, DU_m the modified degree of unsaturation, Cn:1 the FAME with one double bond and number of n carbon atoms in the fatty acid function group, Cn:2 the FAME with two double bonds and number of n carbon atoms in the fatty acid function group, and Cn:3 the FAME with three double bonds and number of n carbon atoms in the fatty acid function group.

Another important specification for biodiesel is oxidation stability, affecting biodiesel quality during storage. The oxidized biodiesel could impair the fuel quality, resulting in bad engine performance. Compared to other factors, FAMEs composition is the most critical factor influencing oxidation stability. The oxidation stability of pure FAMEs tabulated in **Table 4** shows that saturated FAMEs have good oxidation stability, but oxidation stability significantly decreases with increasing carbon double bonds. Moreover, temperature substantially affects oxidation stability. The oxidation stability index is used to check the effect of unsaturated FAMEs on oxidation stability (**Eq. 14**) (Pullen and Saeed, 2014). The higher the oxidation stability index, the lower the oxidation stability.

Table 4.
Oxidation stability of pure FAMEs*.

Pure FAMES	Oxidation stability (h)	
	80 °C	110 °C
C16:0	> 40	> 40
C18:0	> 40	> 40
C18:1	15.1	2.5
C18:2	3.5	1
C18:3	0.4	0.2

* Source: Moser (2009)

Another model used to predict the oxidation stability based on the polyunsaturated FAMEs is presented in **Equation 15** (Park et al., 2008). However, these models only consider the unsaturated FAMEs, while the saturated FAMEs also play a vital role in oxidation stability as they decrease the unsaturation degree. A model based on the carbon double bonds concentrations was developed to predict the oxidation stability at the test temperature of 110 °C, considering both types of FAMEs (**Eqs. 16** and **17**). The data used in the proposed model for the statistical regression were obtained from previous studies (Park et al., 2008; Moser, 2009). Since urea inclusion fractionation removes the saturated FAMEs, it causes the L-FAMEs oxidation stability to decrease (**Fig 12b**). The reduced extent of oxidation stability depended on the saturated FAMEs weight percentages decrease. In biodiesel from most feedstocks, except the highly saturated FAMEs feedstocks, antioxidants must be used to improve the oxidation stability.

$$Oxidation\ stability\ index = 0.02\left(x_{C18:1}\right)+\left(x_{C18:2}\right)+2\left(x_{C18:3}\right) \quad \text{Eq. 14}$$

$$Oxidation\ stability\ = 117.9259/\left(x_{C18:2}+x_{C18:3}\right)+2.5905 \quad \text{Eq. 15}$$

where $x_{C18:1}$ the weight percentage of C18:1, $x_{C18:2}$ the weight percentage of C18:2, and $x_{C18:3}$ the weight percentage of C18:3.

$$Oxidation\ stability = 1.851+37.807\times\exp\left(-1.948\times C_{C=C}\right) \quad \text{Eq. 16}$$

$$C_{C=C} = \left(x_{C18:1}/MW_{C18:1}+2x_{C18:2}/MW_{C18:2}+3x_{C18:3}/MW_{C18:3}\right) / \left(\sum x_{FAME,i}/MW_{FAME,i}\right) \quad \text{Eq. 17}$$

3.7. Emissions evaluation

Biodiesel is similar to diesel fuels and can be directly used in the diesel engine. The biodiesel emissions in diesel engines are essential specifications to evaluate biodiesel's sustainability and effect on the environment. Previous studies showed that biodiesel combustion in a diesel engine reduced the emission of hydrocarbons, carbon monoxide, and particulate matter but increased the emission of nitrogen oxides (Zhu et al., 2011; Menkiel et al., 2014). These changes result from the ester functional groups in biodiesel. The effects of FAMEs structures on biodiesel emissions have been investigated (Zhu et al., 2016), and the findings can be used to evaluate the impact of urea inclusion fractionation on biodiesel emissions in the diesel engine. After urea inclusion fractionation, saturated FAMEs were significantly reduced, and the carbon chain length of the major unsaturated FAMEs was 18. Only chicken fat contained a relatively high amount of C16:1. The summary of the emissions changes after urea inclusion is shown in **Table 5**. As seen, hydrocarbons, carbon monoxides, and particulate matter decreased while the nitrogen oxides emission increased.

4. Conclusions and Prospects

Poor low-temperature performance is the main factor inhibiting the usage of renewable, sustainable biodiesel. CP is the appropriate specification to characterize the low-temperature performance based on the phase changes. Urea inclusion fractionation provides a quick and efficient way to reduce CP by removing the saturated FAMEs. Current methods to reduce CP have limitations that the urea inclusion fractionation method could address while providing better efficiency. Urea inclusion fractionation for reducing CP was evaluated considering various factors: ratios of urea to FAMEs, ratios of methanol to FAMEs, various solvents, various feedstocks, and various operating temperatures. The driving force of urea inclusion fractionation is urea supersaturation in solution, which is influenced by the types of solvents, initial soluble urea fraction, type of FAMEs, and operating temperature. The most significant factor is the initial soluble urea fraction in the solution. The separation efficiency and selectivity depend on the saturation and carbon chain length. Most FAMEs with saturated FAMEs contents below 20% undergo single urea inclusion fractionation to produce L-FAMEs with CP values lower than -18 to -41 °C at 75 to 80% yield. Palm oil FAMEs undergo a double urea inclusion fractionation process to produce L-FAMEs with -17 °C at 46% yield. Besides CP, cetane number and oxidation stability were also predicted by models based on the FAMEs composition. The cetane number was better than the minimum requirement for biodiesel in response to urea inclusion fractionation. Oxidation stability decreased, but it can be improved by

Please cite this article as: Liu J., Tao B. Fractionation of fatty acid methyl esters *via* urea inclusion and its application to improve the low-temperature performance of biodiesel. Biofuel Research Journal 34 (2022) 1617-1629. DOI: 10.18331/BRJ2022.9.2.3

Table 5.
Effect of urea inclusion fractionation on biodiesel emissions.

Baseline fuel for comparison	Engine speed (rpm)	BMEP*	Hydrocarbons	Carbon monoxide	Nitrogen oxides	Particulate matter
Diesel	1200	Low	↓	↓	↑	↓
		High	↓	↓↓	Negligible	↓↓
	2000	Low	↓↓	↓↓	↑	↓↓
		High	↓↓	↓↓	↑	↓↓
Original FAMEs	1200	Low	↓	↓	Negligible	↓
		High	Negligible	↓↓	Negligible	↓
	2000	Low	↓	↓	↑	↓
		High	↓	↓↓	↑	↓

* BMEP: brake mean effective pressure

adding antioxidants. After urea inclusion fractionation, L-FAMEs tend to cause lower emissions of hydrocarbons, carbon monoxides, and particulate matter but increased emission of nitrogen oxides.

Urea inclusion fractionation provides a way to make the unsaturated FAMEs enriched mixtures. Besides being winter season biodiesel, these FAMEs can also be used as feedstocks for chemicals production, such as estolides as bio-lubricants through epoxidation.

Acknowledgements

This work was financially supported by Indiana Soybean Alliance.

References

[1] Atabani, A.E., Silitonga, A.S., Badruddin, I.A., Mahlia, T.M.I., Masjuki, H.H., Mekhilef, S., 2012. A comprehensive review on biodiesel as an alternative energy resource and its characteristics. Renew. Sust. Energy Rev. 16(4), 2070-2093.

[2] Bai, H., Tian, J., Talifu, D., Okitsu, K., Abulizi, A., 2022. Process optimization of esterification for deacidification in waste cooking oil: RSM approach and for biodiesel production assisted with ultrasonic and solvent. Fuel, 318, 123697.

[3] Bi, Y., Ding, D., Wang, D., 2010. Low-melting-point biodiesel derived from corn oil via urea complexation. Bioresour. Technol. 101(4), 1220-1226.

[4] Bist, S., Tao, B.Y., Mohtar, S., 2009. Method for separating saturated and unsaturated fatty acid esters and use of separated fatty acid esters. US20090199462A1.

[5] Boey, P.L., Maniam, G.P., Hamid, S.A., 2009. Biodiesel production via transesterification of palm olein using waste mud crab (*Scylla serrata*) shell as a heterogeneous catalyst. Bioresour. Technol. 100(24), 6362-6368.

[6] Bouaid, A., Hahati, K., Martinez, M., Aracil, J., 2014. Biodiesel production from biobutanol. improvement of cold flow properties. Chem. Eng. J. 238, 234-241.

[7] Cardoso, C.C., Celante, V.G., De Castro, E.V.R., Pasa, V.M.D., 2014. Comparison of the properties of special biofuels from palm oil and its fractions synthesized with various alcohols. Fuel. 135, 406-412.

[8] Cetinkaya, M., Karaosmanoğlu, F., 2004. Optimization of base-catalyzed transesterification reaction of used cooking oil. Energy Fuels. 18(6), 1888-1895.

[9] Chiu, C.W., Schumacher, L.G., Suppes, G.J., 2004. Impact of cold flow improvers on soybean biodiesel blend. Biomass Bioenergy. 27(5), 485-491.

[10] Dunn, R.O., 2009. Effects of minor constituents on cold flow properties and performance of biodiesel. Prog. Energy Combust. Sci. 35(6), 481-489.

[11] Dunn, R.O., Shockley, M.W., Bagby, M.O., 1997. Winterized methyl esters from soybean oil: an alternative diesel fuel with improved low-temperature flow properties. SAE Trans. 640-649.

[12] Dunn, R.O., 2011. Improving the cold flow properties of biodiesel by fractionation, in: Ng, T.-B. (Ed.), Soybean - Applications and Technology. Intech. Croatia, pp. 211-240.

[13] Foon, C.S., Liang, Y.C., Lida, N., Mat, H., May, C.Y., Institusi, P., Bangi, B.B., Pantai, L., Lumpur, K., 2006. Crystallisation and Melting Behavior of Methyl Esters of Palm Oil. Am. J. Appl. Sci. 3(5), 1859-1863.

[14] González Gómez, M.G., Howard-Hildige, R., Leahy, J.J., Rice, B., 2002. Winterisation of waste cooking oil methyl ester to improve cold temperature fuel properties. Fuel. 81(1), 33-39.

[15] Hayes, D.G., Bengtsson, Y.C., Van Alstine, J.M., Setterwall, F., 1998. Urea complexation for the rapid, ecologically responsible fractionation of fatty acids from seed oil. J. Am. Oil Chem. Soc. 75(10), 1403-1409.

[16] Hazrat, M.A., Rasul, M.G., Mofijur, M., Khan, M.M.K., Djavanroodi, F., Azad, A.K., Bhuiya, M.M.K., Silitonga, A.S., 2020. A mini review on the cold flow properties of biodiesel and its blends. Front. Energy Res. 326.

[17] Imahara, H., Minami, E., Hari, S., Saka, S., 2008. Thermal stability of biodiesel in supercritical methanol. Fuel. 87(1), 1-6.

[18] Kalligeros, S., Zannikos, F., Stournas, S., Lois, E., Anastopoulos, G., Teas, C., Sakellaropoulos, F., 2003. An investigation of using biodiesel/marine diesel blends on the performance of a stationary diesel engine. Biomass Bioenergy. 24(2), 141-149.

[19] Lapuerta, M., Rodríguez-Fernández, J., Fernández-Rodríguez, D., Patiño-Camino, R., 2018. Cold flow and filterability properties of n-butanol and ethanol blends with diesel and biodiesel fuels. Fuel. 224, 552-559.

[20] Lee, F.M., Lahti, L.E., 1972. Solubility of urea in water-alcohol mixtures. J. Chem. Eng. Data 17(3), 304-306.

[21] Lee, I., Johnson, L.A., Hammond, E.G., 1996. Reducing the crystallization temperature of biodiesel by winterizing methyl soyate. J. Am. Oil Chem. Soc. 73(5), 631-636.

[22] Lee, Y.H., Choi, K.S., Jang, Y.S., Shin, J.A., Lee, K.T., Choi, I.H., 2014. Improvement of Low-temperature fluidity of biodiesel from vegetable oils and animal fats using urea for reduction of total saturated FAME. J. Korean Appl. Sci. Technol. 31(1), 113-119.

[23] McCormick, R., 2006. DOE / GO-102006-2358 Third Edition September 2006.

[24] Menkiel, B., Donkerbroek, A., Uitz, R., Cracknell, R., Ganippa, L., 2014. Combustion and soot processes of diesel and rapeseed methyl ester in an optical diesel engine. Fuel. 118, 406-415.

[25] Mishra, S., Anand, K., Mehta, P.S., 2016. Predicting the Cetane Number of Biodiesel Fuels from Their Fatty Acid Methyl Ester Composition. Energy Fuels. 30(12), 10425-10434.

[26] Monthly Energy Review, 2022. U.S. Energy Information Administration.

[27] Monthly Biodiesel Production Report, 2021. U.S. Energy Information Administration.

[28] Moser, B.R., 2009. Comparative oxidative stability of fatty acid alkyl esters by accelerated methods. J. Am. Oil Chem. Soc. 86(7), 699-706.

[29] Nainwal, S., Sharma, N., Sharma, A. Sen, Jain, Shivani, Jain, Siddharth, 2015. Cold flow properties improvement of Jatropha curcas biodiesel and waste cooking oil biodiesel using winterization and blending. Energy. 89, 702-707.

Please cite this article as: Liu J., Tao B. Fractionation of fatty acid methyl esters *via* urea inclusion and its application to improve the low-temperature performance of biodiesel. Biofuel Research Journal 34 (2022) 1617-1629. DOI: 10.18331/BRJ2022.9.2.3

[30] Nowatzki, J., Shrestha, D., Swenson, A., Wiesenborn, D., 2019. Biodiesel cloud point and cold weather issues. Farm-Energy.

[31] Park, J.Y., Kim, D.K., Lee, J.P., Park, S.C., Kim, Y.J., Lee, J.S., 2008. Blending effects of biodiesels on oxidation stability and low temperature flow properties. Bioresour. Technol. 99(5), 1196-1203.

[32] Pullen, J., Saeed, K., 2014. Experimental study of the factors affecting the oxidation stability of biodiesel FAME fuels. Fuel Process. Technol. 125, 223-235.

[33] Rashid, U., Anwar, F., 2008. Production of biodiesel through optimized alkaline-catalyzed transesterification of rapeseed oil. Fuel. 87(3), 265-273.

[34] Schlenk, H., 1954. Urea inclusion compounds of fatty acids. Prog. Chem. Fats Other Lipids. 2, 243-246.

[35] Senra, M., McCartney, S.N., Soh, L., 2019. The effect of bio-derived additives on fatty acid methyl esters for improved biodiesel cold flow properties. Fuel. 242, 719-727.

[36] Sharma, Y.C., Singh, B., 2009. Development of biodiesel: Current scenario. Renew. Sust. Energy Rev. 13(6–7), 1646–1651.

[37] Shrestha, D.S., Van Gerpen, J., Thompson, J., 2008. Effectiveness of cold flow additives on various biodiesels, diesel, and their blends. Trans. ASABE. 51(4), 1365-1370.

[38] Sierra-Cantor, J.F., Guerrero-Fajardo, C.A., 2017. Methods for improving the cold flow properties of biodiesel with high saturated fatty acids content: a review. Renew. Sust. Energy Rev. 72, 774-790.

[39] Silitonga, A.S., Ong, H.C., Mahlia, T.M.I., Masjuki, H.H., Chong, W.T., 2014. Biodiesel conversion from high FFA crude *Jatropha curcas*, *Calophyllum inophyllum* and *Ceiba pentandra* oil. Energy Procedia. 61, 480-483.

[40] Smith, P.C., Ngothai, Y., Nguyen, Q.D., O'Neill, B.K., 2009. Alkoxylation of biodiesel and its impact on low-temperature properties. Fuel. 88(4), 605-612.

[41] Su, Y.C., Liu, Y.A., Diaz Tovar, C.A., Gani, R., 2011. Selection of prediction methods for thermophysical properties for process modeling and product design of biodiesel manufacturing. Ind. Eng. Chem. Res., 50(11), 6809–6836.

[42] Tajima, H., Abe, M., Komatsu, H., Yamagiwa, K., 2021. Feasibility of additive winterization of biodiesel fuel derived from various eatable oils and fat. Fuel. 305, 121479.

[43] Tang, H., Salley, S.O., Ng, K.S., 2008. Fuel properties and precipitate formation at low temperature in soy-, cottonseed-, and poultry fat-based biodiesel blends. Fuel. 87(13-14), 3006-3017.

[44] Thurston, G.D., 2022. Fossil fuel combustion and PM2.5 mass air pollution associations with mortality. Environ. Int. 160, 107066.

[45] Vohra, K., Vodonos, A., Schwartz, J., Marais, E.A., Sulprizio, M.P., Mickley, L.J., 2021. Global mortality from outdoor fine particle pollution generated by fossil fuel combustion: results from GEOS-Chem. Environ. Res. 195, 110754.

[46] Wang, X., Xiaohan, W., Chen, Y., Jin, W., Jin, Q., Wang, X., 2020. Enrichment of branched chain fatty acids from lanolin via urea complexation for infant formula use. LWT. 117, 108627.

[47] Yeong, S.P., San Chan, Y., Law, M.C., Ling, J.K.U., 2021. Improving cold flow properties of palm fatty acid distillate biodiesel through vacuum distillation. J. Bioresour. Bioprod. 7(1), 43-51.

[48] Yovany Benavides, A., Benjumea, P.N., Agudelo, J.R., 2008. El fraccionamiento por cristalización del biodiesel de aceite de palma como alternativa para mejorar sus propiedades de flujo a baja temperature. Rev. Facultad. Ing. Universidad Antioquia. (43), 07-17.

[49] Zhu, L., Cheung, C.S., Huang, Z., 2016. Impact of chemical structure of individual fatty acid esters on combustion and emission characteristics of diesel engine. Energy. 107, 305-320.

[50] Zhu, L., Cheung, C.S., Zhang, W.G., Huang, Z., 2011. Combustion, performance and emission characteristics of a di diesel engine fueled with ethanol-biodiesel blends. Fuel. 90(5), 1743-1750.

Dr. Junli Liu obtained his PhD degree in the field of Agricultural and Biological Engineering from Purdue University in 2012. His PhD dissertation was on biodiesel fractionation and process simulation and optimization. He worked in the biodiesel industry from 2013 to 2016 after graduation and was in charge of the company's research and development and process development. In addition, he was a BQ-9000 committee member in the company and was responsible for biodiesel production quality control. He worked as a research scientist at Purdue University to develop biosorbents and nanomaterials from hemp from 2016 to 2018. He became a researcher at the University of Illinois at Urbana Champaign in 2019 and developed a novel ultrasonic separation/purification for fermented aqueous ethanol. Dr. Junli Liu is a lecturer at Purdue University now, and his scientific research interests and experience include biofuel, bioenergy, biomaterials, wastewater treatment, desalting, separation, modelling and simulation, and nanotechnology.

Dr. Bernard Tao completed his PhD degree at the Iowa State University in 1988. Then, he became a faculty at Purdue University. He has made enormous impacts through his work with the Indiana Soybean Alliance, especially in founding and growing the Student Soybean Innovation Competition. This competition has provided hundreds of Purdue students with invaluable practical experiences in innovation that launched numerous products and life-long innovators and entrepreneurs into their careers around the US and the world. In addition, his research in soybean utilization resulted in numerous innovations that have led to wider use of soybeans in biofuels, biopolymers, crayons, candles, concrete sealant, and more. Dr. Bernard Tao holds more than 11 US patents and his research interest includes biopolymer, biofuels, genetic engineering, and lipid-carbohydrate polymers.

Please cite this article as: Liu J., Tao B. Fractionation of fatty acid methyl esters *via* urea inclusion and its application to improve the low-temperature performance of biodiesel. Biofuel Research Journal 34 (2022) 1617-1629. DOI: 10.18331/BRJ2022.9.2.3